Journal of Organometallic Chemistry 864 (2018) 143–147

Contents lists available at ScienceDirect

Journal of Organometallic Chemistry

journal homepage: www.elsevier.com/locate/jorganchem

Nickel bis(dithiolene) complexes for electrocatalytic hydrogen evolution: A computational study

Zisheng Zhang [b], Tilong Yang [b], Peng Qin [a], Li Dang [a, b, *]

[a] Department of Chemistry and Key Laboratory for Preparation and Application of Ordered Structural Materials of Guangdong Province, Shantou University, Guangdong, 515063, PR China
[b] Department of Chemistry, Southern University of Science and Technology, Shenzhen, 518055, PR China

ARTICLE INFO

Article history:
Received 30 October 2017
Received in revised form
5 March 2018
Accepted 5 March 2018
Available online 16 March 2018

Keywords:
Reaction mechanism
DFT calculation
Non-innocent complex
Hydrogen evolution reaction
Ligand effects

ABSTRACT

The substituent effect of dithiolene ligand on electrocatalytic activity of Ni bis(dithiolene) towards hydrogen evolution reaction (HER) are thoroughly explored with computational methods. A series of differently substituted dithiolene ligands are compared and evaluated. These computational results indicate that adding electron-withdrawing groups on the ligand or enlarging the conjugate Π system of the ligand can greatly reduce the reduction potentials, while tuning the electronic structure of the non-innocent framework can optimize the geometry of dihydrogen species to achieve lower energy barrier for H_2 elimination. This study may benefit the deep understanding of the electrocatalyzed HER mechanism and give inspirations on the design of efficient nickel bis(dithiolene) electrocatalysts with low overpotential and improved kinetics.

1. Introduction

Hydrogen, considered as the ideal energy resource for its extremely high energy density and environmental-friendly chemical composition [1], has aroused much research interest. However, the high kinetic barrier for deriving hydrogen from water by HER (Hydrogen Evolution Reaction) makes the large-scale production and application of hydrogen extremely hard [2]. To go around this difficulty, scientists have been exploring electrocatalysts that can replace the direct hydrogen electrolysis process with a series of reduction and protonation steps which possess much lower energy barrier [3]. Due to the high price and limited reserve of noble metal electrocatalysts, electrocatalysts based on earth-abundant elements with low the redox potential to drive HER and increases the turnover frequency is nowadays a hot research topic [4]. Among the various transition metal-based electrocatalysts [5–12], nickel bis(-dithiolene) complexes are attracting increasing interests. Featured in its electron-rich metal center and non-innocent bidentate ligands, nickel bis(dithiolene) complex has already been intensely studied in olefin purification [13], with deep understanding of its related mechanism [14–16]. Recent study also showed that nickel dithiolene complexes exhibit activity in electrocatalytic and photocatalytic HER [17–19]. In this article, inspired by previous work [20–22], we proposed a revised electrochemical mechanism which does not only fit well with reported experimental results, but also provide rich theoretical insights. To carry out an analysis of exact and detailed mechanism by considering both the kinetics and thermodynamics, we applied DFT computations to explore the substituent effects on electronic structures, geometry, electrocatalytic activity of various nickel bis(dithiolene) complexes.

2. Computational details

DFT computations were performed using the Gaussian 09 program [23]. ω-B97XD functional [24] is adopted for its long-range exchange and empirical dispersion corrections which make it widely accepted as proper functional to study structure transition metal dithiolene reactions [13]. The LanL2DZ basis set, containing double-ξ valence with effective core potentials (ECPs) of Hay and Wadt, was used for Ni atoms [25–28]. Polarization functions were also added to Ni (f = 3.130) [29,30] for better precision. For all other atoms including H, C, N, F and S, 6-311+G** basis set [31–33] was used. The geometric structures of all species were optimized in the

* Corresponding author. Department of Chemistry and Key Laboratory for Preparation and Application of Ordered Structural Materials of Guangdong Province, Shantou University, Guangdong, 515063, PR China.
E-mail address: ldang@stu.edu.cn (L. Dang).

https://doi.org/10.1016/j.jorganchem.2018.03.007
0022-328X/

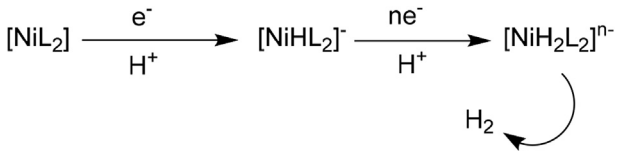

Fig. 1. Hydrogen evolution from electronic reduction of protons through Ni complexes.

gas phase. Harmonic vibrational frequencies were also computed, whose result showed that all reaction intermediates have no imaginary frequency and each transition state has only one imaginary frequency. Solvation corrections were computed B3LYP functional [34] and the basis sets used in gas phase optimization, based on the gas-phased optimized geometries. SMD (Solvation Model Density) [35] was adopted, with N,N-Dimethylformamide being the solvent. Solvation-corrected Gibbs energy values of high-spin and low-spin forms of all intermediates were calculated, and the more stable one is regarded as the actual present species which were then used in the calculation. Molecular orbital compositions and oxidation states were analyzed by Hirshfeld method and LOBA method respectively as implemented in Multiwfn [36].

The acid dissociation energies were computed in respect to the CF_3COOH/CF_3COO couple, and the standard redox potential was obtained with reduction potential of ferrocene couple as a reference:

$$E^o(A)\ vs\ \left(Fc/Fc^+\right) = \frac{\left[G_{sol}(Fc) - G_{sol}\left(Fc^+\right)\right] - \left[G_{sol}\left(A^-\right) - G_{sol}(A)\right]}{nF}$$

In this relation, G_{sol} is the computed Gibbs energy of a species after solvation correction and F is the Faraday constant. Since only one-electron reduction steps are involved, for all reduction steps: $n = 1$.

3. Results and discussion

In the first part of this study we proposed a detailed mechanism for electrocatalytic HER using nickel bis(dithiolene) complexes. In the second part, we explored the electrochemical steps of different nickel bis(dithiolene) complexes and provided an activity descriptor for electrocatalytic activity.

The electrocatalytic mechanism of hydrogen evolution using nickel bis(dithiolene) (denoted as **[NiL$_2$]**, **L** is a dithiolene ligand) stays elusive due to the complicated multi-step process and various possible pathways. As is shown in Fig. 1, the neutral starting species **[NiL$_2$]** goes through a reduction-protonation or protonation-reduction pathway to **[NiHL$_2$]$^-$**. Then the monoanion undergoes a protonation step and several reduction steps, in unknown sequence, to become **[NiH$_2$L$_2$]$^{n-}$** (charge unknown) which finally releases a hydrogen molecule via reductive elimination. The complexity in possible pathways and intermediates makes the exploration of a general mechanism for such reaction rather difficult.

3.1. Mechanism exploration

To gain insight into the general mechanism for electrocatalytic hydrogen evolution using nickel bis(dithiolene), a range of nickel bis(dithiolene) complexes with different substituents on the ligands were designed (Fig. 2). Thermodynamics and geometric structures were calculated to obtain information to determine the most feasible pathway.

Based on the calculations, an optimized mechanism can be proposed as shown in Fig. 3. For convenience, reduction steps and protonation steps are denoted as ET and PT, respectively. In the first step, **[NiL$_2$]** is reduced to **[NiL$_2$]$^-$**. The second step is the reduction of **[NiL$_2$]$^-$** to **[NiL$_2$]$^{2-}$**, because protonation of **[NiL$_2$]$^-$** to **[NiHL$_2$]$^-$** is impossible for its weak basicity. **[NiHL$_2$]$^-$** is protonated again to **[NiH$_2$L$_2$]** rather than being reduced since the redox potential of **[NiHL$_2$]$^-$** to **[NiHL$_2$]$^{2-}$** is too negative. **[NiHL$_2$]$^{2-}$** is then protonated to form **[NiH$_2$L$_2$]$^-$** which releases hydrogen in the final reductive elimination. During the ET-ET-PT process, bond length of C-C and Ni-S decreased slightly while those of C-S increased, suggesting the weakening of C=S character and enhanced interaction between S and Ni. The dihedral angles between two ligands in the intermediates increased slightly as each electron transferred, but the geometry remains square planar at the nickel center. Bond length of involved S-H were all calculated to be 1.35 Å, showing the stability of proton on the non-innocent framework. It is worth noting that the geometry of the complex transformed to a semi-tetrahedral structure after the third ET step. The shift in hybridization mode lead to decreased S-Ni bond length in **[NiHL$_2$]$^{2-}$** and **[NiH$_2$L$_2$]$^-$**. Hydrogen evolution from the reductive elimination (RE) of **[NiH$_2$L$_2$]$^-$** is therefore thermodynamically favored due to this geometry change. However, hydrogen evolution from the RE of

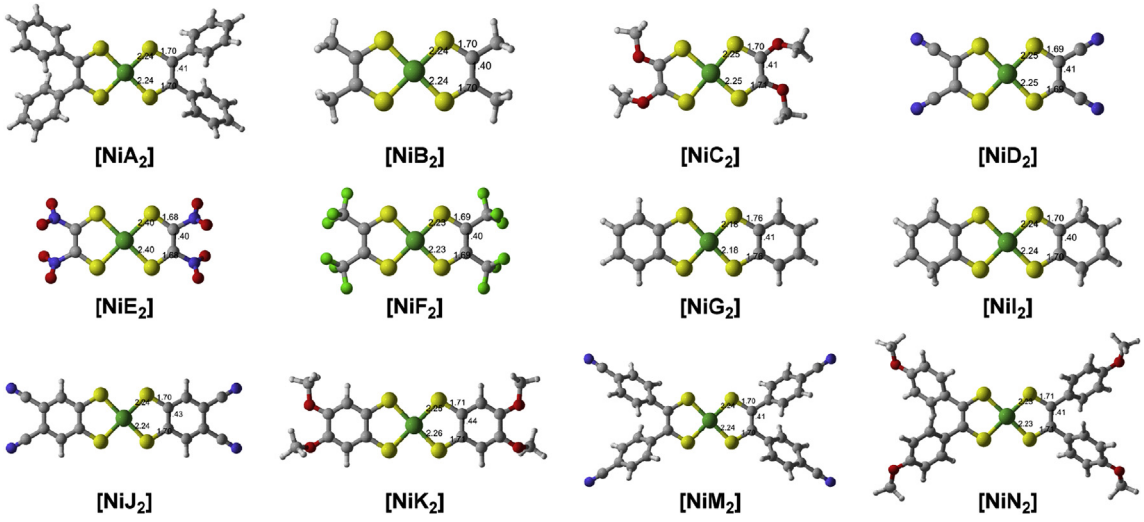

Fig. 2. The designed nickel bis(dithiolene) complexes.

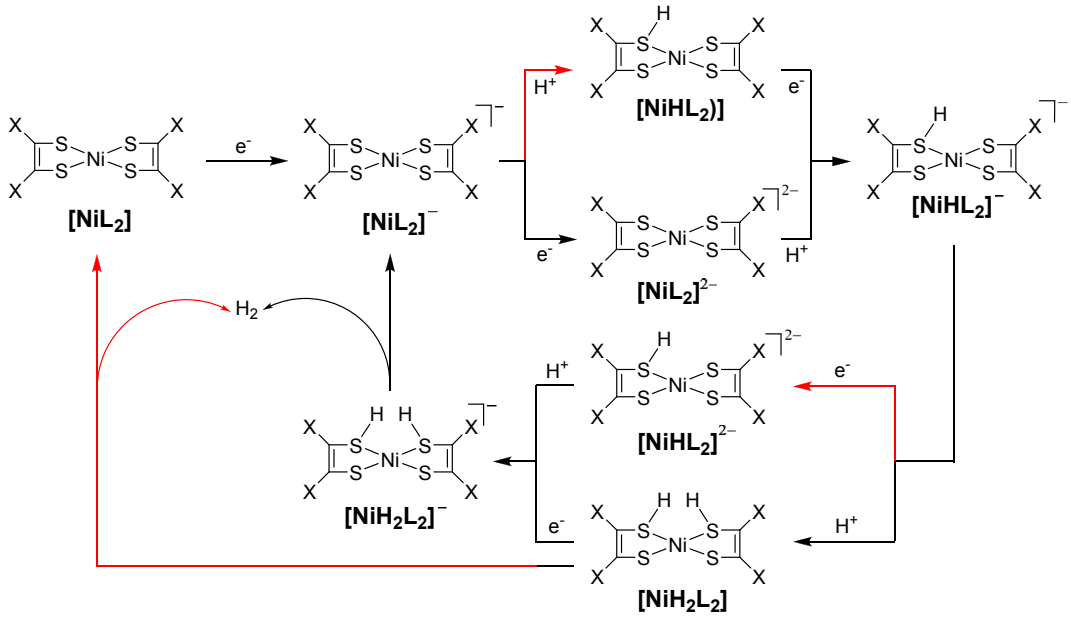

Fig. 3. All possible reaction pathways for electrocatalytic hydrogen evolution using nickel bis(dithiolene) complexes. Red arrows stand for thermodynamically unfavored pathways. (For interpretation of the references to colour in this figure legend, the reader is referred to the web version of this article.)

Table 1
The percentage contribution of Ni, S and C orbitals to the non-innocent framework in HOMO of all investigated nickel bis(dithiolene) complexes as well as pKa and ligand constant of their corresponding dithiolene ligands.

Ligand in [NiL$_2$]	Ni[a] (%)	S[a] (%)	C[a] (%)	pK_a[b]
A	9.77	59.32	30.91	8.50
B	10.57	60.15	29.28	8.75
C	8.31	58.37	33.32	7.97
D	10.26	62.42	27.32	5.89
E	15.01	79.06	5.93	5.81
F	11.44	61.97	26.59	6.60
G	10.93	62.56	26.51	8.00
I	10.88	60.15	28.97	8.71
J	12.07	64.90	23.03	6.72
K	10.00	64.12	25.88	8.09
M	10.33	59.56	30.11	8.01
N	9.72	57.88	32.40	9.34

[a] Orbital contributions of Ni, S and C to the non-innocent framework in HOMO of [NiL$_2$] complexes (L = A ~ N, respectively) were analyzed by Hirshfeld method.
[b] pKa was calculated with reference to TFA at 25 °C.

[NiH$_2$A$_2$] was thermodynamically unfavored (or even blocked) since it remained a square planar geometry in which two hydrogen atoms are confined far apart. In summary, the most feasible pathway is found to be (ET-)ET-PT-PT-ET-RE, with **[NiL$_2$]$^-$** mono-anion being the real active electrocatalytic species. The calculated electrochemical parameters are within 100 mV deviation from previously reported values [20] for a characteristic complex **[NiA$_2$]**, proving the validity of the computational method. The mechanism applies to other investigated nickel bis(dithiolene) electrocatalysts in this study, and all results were summarized in Fig. S2.

The mechanism is quite different from that of cobalt dithiolenes, which is caused by structural difference between **[CoH$_2$L$_2$]** and **[NiH$_2$L$_2$]** intermediates. In the hydrogen evolution cycle using cobalt dithiolenes, Co-H intermediate is involved and the deprotonated (Co-H)(S-H) species releases hydrogen gas, which is due to the high contribution of Co orbitals in the non-innocent framework (basic dithiolene structure and one metal center) [37]. However, as is shown in Table 1, the contribution of Ni orbitals to the non-innocent framework in HOMO is much lower than that of sulfur atoms for all investigated nickel bis(dithiolene) complexes. In

Table 2
Calculated redox potential (vs. Fc$^{+/0}$) and p*K*a for electrochemical steps in the proposed hydrogen evolution mechanism for [NiL$_2$] electrocatalysts with different ligands. The Gibbs free energy change and the lowest redox potential for overall reaction (E$_{(overall)}$) in all electrocatalysts under this study are also provided.

Ligand in [NiL$_2$]	E(ET$_0$)[a] (V)	E(ET$_1$)[a] (V)	pK_a(PT$_1$)[b]	pK_a(PT$_2$)[b]	E(ET$_2$)[a] (V)	ΔG(R.E.) (kcal/mol)	E(overall)[c] (V)
A	−0.36	−1.31	6.76	6.11	−1.33	−20.63	−1.33
B	−0.61	−1.38	7.32	6.30	−1.50	−21.98	−1.50
C	−0.86	−1.29	6.73	5.60	−1.15	−19.26	−1.29
D	0.66	−0.38	4.38	3.48	−0.58	−10.48	−0.58
E	0.73	−0.14	4.23	3.13	−0.29	−1.12	−0.29
F	0.56	−0.69	5.04	3.78	−0.75	−16.19	−0.75
G	0.47	−0.99	6.43	5.89	−1.32	−16.10	−1.32
I	−0.04	−1.04	7.42	6.69	−1.41	−9.24	−1.41
J	0.59	−0.57	5.11	4.57	−1.01	−14.35	−1.01
K	−0.28	−1.09	6.58	6.83	−1.59	−18.46	−1.59
M	−0.17	−1.10	6.40	5.29	−1.14	−18.12	−1.14
N	−0.90	−1.34	7.55	7.03	−1.43	−13.73	−1.43

[a] Redox potential was calculated with reference to Fc$^{+/0}$.
[b] pK_a was calculated with reference to TFA at 25 °C.
[c] The most positive potential needed to drive the overall hydrogen evolution reaction according to proposed mechanism.

addition, LOBA analysis suggest that oxidation states of nickel in **[NiL$_2$]**, **[NiL$_2$]**$^-$ and **[NiL$_2$]**$^{2-}$ remain +2 regardless of the total charge of the species. Both results strongly suggest that in nickel bis(dithiolene) complexes the protonation and redox events take place on the ligand framework, and the non-innocent sulfur atoms are the real catalytic sites.

3.2. Substituent effects on electrochemical reactivity

With the optimal hydrogen evolution mechanism revealed, we can evaluate the performance of a **[NiL$_2$]** electrocatalyst by calculating redox potential, pK_a and ΔG of electrochemical steps in the proposed (ET-)ET-PT-PT-ET-RE pathway. Calculations were performed on all **[NiL$_2$]** electrocatalyst with **A-N** ligands (Table 2). The most positive potentials are critical to drive the overall electrocatalytic reaction, as a criterion to evaluate electrocatalytic activity, redox potentials and pK_a values are also summarized in Table 2.

From Table 2, it is obvious that substituent on dithiolene ligands has effect on electrocatalytic activity of **[NiL$_2$]** electrocatalysts. Electron withdrawing groups can reduce the lowest redox potential when compare with electron donating or neutral groups. Electron withdrawing groups increase the electron density of S atoms in the non-innocent frameworks (Table 1), leading to a larger contribution of sulfur atoms to HOMO of Ni bis(dithiolene). Since sulfur atoms are the active sites in the non-innocent framework, enlarging their orbital contribution would enhance the electrocatalytic activity of the species.

Table 2A–F shows calculated redox potential (vs. Fc+/0) and pK_a for electrochemical steps. From the results, we can see that substituting electron-withdrawing groups (EWG) on dithiolene ligand can enhance the electroredox activity while electron-donating groups (EDG) do the opposite job. Substitutes with Hyperconjugation (**B**), Conjugation (**A**) and inductive (**C**) electron-donating effects all lead to poor electrocatalytic activity. Inductive electron-withdrawing effect (**F**) results in a boost in performance, however, the boost is not as drastic as those resulted from conjugation electron-withdrawing effects (**D** and **E**). The difference is understandable because the non-innocent conjugation system mainly consists of unbonded p orbitals of S atoms. Conjugation electronic effect induces a much more direct change in electron density in p orbitals of S than inductive effect, therefore leading to a more obvious enhancement in electrocatalytic activity.

Introduction of aromatic structure was found beneficial compared to simple alkyl-substituted dithiolene ligands. **A** and **G** exhibit better performance than **B** and **I**, respectively. Substituting functional groups to aromatic systems induces similar changes as those on simple dithiolene structures (**J**, **K**, **M** and **N**), but the effect on electrocatalytic activity is not obvious.

Our calculations of hydrogen evolution using as-designed nickel bis(dithiolene) show that dihydrogen is formed from two S-H groups rather than from one Ni-H and one S-H group since Ni-H complex is quite unstable as has been found in our previous study of MoS_2 catalyzed HER [12]. To further understand the substituent effects on this dihydrogen elimination process, we calculated the energy barriers for all compounds investigated in this study. The computed values, ranging from 27.4 kcal/mol to 41.9 kcal/mol, may seem too large for a feasible hydrogen evolution. However, several compounds with calculated energy barriers ranging from 35 kcal/mol to 40 kcal/mol have been previously reported to be able to drive electrocatalytic HER [20,22]. We believe that some other factors may be in effect that make this dihydrogen elimination process feasible. Interfacial adsorptions, solvation effect and electrode kinetics may contribute to such a phenomenon, and they deserve more precise modeling of electrocatalysis in realistic conditions.

From Fig. 4 (a) and (b), it is obvious that the direct or indirect introduction of electron-withdrawing groups to the non-innocent framework can result in a higher energy barrier, probably due to the change in electronic structure of the central nickel atom. Electron-deficient non-innocent framework gives rise to a less distorted geometry of the **[NiH$_2$L$_2$]**$^-$ species in which two captured hydrogen atoms are spatially separated (see SI). However, the compounds presented in (c) do not follow this trend. It can be seen that the removal of aromaticity (**G**) will create a higher energy barrier that is rather difficult to overcome, compared to its aromatic counterpart. The introduction of electron-withdrawing groups, surprisingly, leads to a lower energy barrier, possibly because the involvement of benzene structure alters the orbital properties over the non-innocent framework.

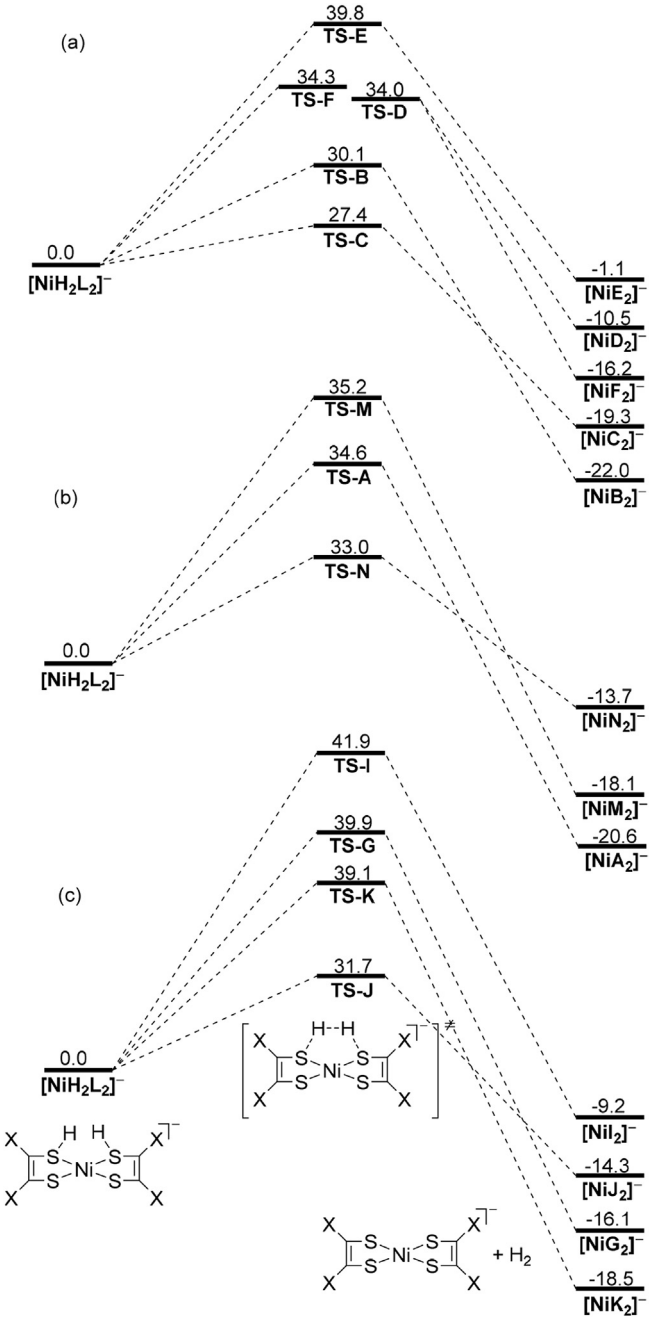

Fig. 4. Energy profile for the dihydrogen elimination process of (a) **B**, **C**, **D**, **E**, **F**, (b) **A**, **M**, **N** and (c) **G**, **I**, **K**, **L**. The compounds are grouped according to similar structure of non-innocent frameworks that they are based upon.

The effort to cut down the required potential and the endeavor to look for pathways with lower energy barrier, according to our calculations above, appear to be contradictory to each other in some extent. The elusive balance between two goals, namely high electroredox activity and good optimized geometry, may be achieved by tuning the electronic structures of the non-innocent framework. To master this subtle molecular engineering, more extensive and insightful theoretical understanding of this system is still required.

4. Conclusions

Computational investigations of electrocatalytic hydrogen evolution process using nickel bis(dithiolene) complexes revealed the most feasible reaction pathway. The sulfur atoms in non-innocent framework, showing high contribution to HOMO, were found to be the real catalytic sites where reductions and protonations take place. By making modifications to the ligands, orbital compositions can be affected and therefore the electrochemical activity. Different electronic effects of introduced substituents were analyzed, as well as their influence on electrocatalytic activity and energy barriers of dihydrogen elimination step. The conjugation electron-withdrawing effect was found most beneficial for the electrocatalytic process. The contradiction between high electroredox activity and hydrogen evolution kinetics is analyzed, with its origin in electronic structure of non-innocent frameworks discussed. The mechanistic investigation gives insight into the electrocatalytic process and puts forward the electronic structure problem underlying the electrocatalysis, which may pave the way for rational design of nickel bis(dithiolene) electrocatalysts for HER.

Acknowledgements

Financial supports from the National Natural Science Foundation of China (No. 21573102) and Department of Education of Guangdong Province are appreciated.

Appendix A. Supplementary data

Complete Reference 23, Tables of calculated redox potential and pKa values, the optimized structures and Cartesian coordinate for all species.

Supplementary data related to this article can be found at https://doi.org/10.1016/j.jorganchem.2018.03.007.

References

[1] S. Dutta, J. Ind. Eng. Chem. 20 (2014) 1148–1156.
[2] R.M. Bullock, A.M. Appel, M.L. Helm, Chem. Commun. 50 (2014) 3125–3143.
[3] F. Safizadeh, E. Ghali, G. Houlachi, Int. J. Hydrogen Energy 40 (2015) 256–274.
[4] B. Ginovska-Pangovska, A. Dutta, M.L. Reback, J.C. Linehan, W.J. Shaw, Acc. Chem. Res. 47 (2014) 2621–2630.
[5] W.-F. Chen, J.T. Muckerman, E. Fujita, Chem. Commun. 49 (2013) 8896–8909.
[6] X. Hu, B.S. Brunschwig, J.C. Peters, J. Am. Chem. Soc. 129 (2007) 8988–8998.
[7] V.S. Thoi, Y. Sun, J.R. Long, C.J. Chang, Chem. Soc. Rev. 42 (2013) 2388–2400.
[8] P.-A. Jacques, V. Artero, J. Pécaut, M. Fontecave, Proc. Natl. Acad. Sci. Unit. States Am. 106 (2009) 20627–20632.
[9] J.R. McKone, S.C. Marinescu, B.S. Brunschwig, J.R. Winkler, H.B. Gray, Chem. Sci. 5 (2014) 865–878.
[10] M. Gong, D.Y. Wang, C.C. Chen, B.J. Hwang, H. Dai, Nano Research 9 (2016) 28–46.
[11] W. Lubitz, H. Ogata, O. Rüdiger, E. Reijerse, Chem. Rev. 114 (2014) 4081–4148.
[12] T.-L. Yang, S.-F. Ni, P. Qin, L. Dang, Chem. Commun. 54 (2018) 1113–1116.
[13] H. Li, E.N. Brothers, M.B. Hall, Inorg. Chem. 53 (2014) 9679–9691.
[14] D.J. Harrison, N. Nguyen, A.J. Lough, U. Fekl, J. Am. Chem. Soc. 128 (2006) 11026–11027.
[15] L. Dang, M.F. Shibl, X. Yang, A. Alak, D.J. Harrison, U. Fekl, E.N. Brothers, M.B. Hall, J. Am. Chem. Soc. 134 (2012) 4481–4484.
[16] L. Dang, M.F. Shibl, X. Yang, D.J. Harrison, A. Alak, A.J. Lough, U. Fekl, E.N. Brothers, M.B. Hall, Inorg. Chem. 52 (2013) 3711–3723.
[17] H. Rao, Z.-Y. Wang, H.-Q. Zheng, X.-B. Wang, C.-M. Pan, Y.-T. Fan, H.-W. Hou, Catal. Sci. Eng. 5 (2015) 2332–2339.
[18] A. Das, Z. Han, W.W. Brennessel, P.L. Holland, R. Eisenberg, ACS Catal. 5 (2015) 1397–1406.
[19] K. Wang, Dithiolene Chemistry, John Wiley & Sons, Inc., 2004, pp. 267–314.
[20] A. Zarkadoulas, M.J. Field, C. Papatriantafyllopoulou, J. Fize, V. Artero, C.A. Mitsopoulou, Inorg. Chem. 55 (2016) 432–444.
[21] Q. Tang, Z. Zhou, J. Phys. Chem. C 117 (2013) 14125–14129.
[22] A. Zarkadoulas, M.J. Field, V. Artero, C.A. Mitsopoulou, ChemCatChem 9 (2017) 2308–2317.
[23] M.J. Frisch, et al., Gaussian 09, Gaussian, Inc., Wallingford CT, 2009.
[24] J. Chai, M. Head-Gordon, Phys. Chem. Chem. Phys. 10 (2008) 6615–6620.
[25] P.J. Hay, W.R. Wadt, J. Chem. Phys. 82 (1985) 270–283.
[26] P.J. Hay, W.R. Wadt, J. Chem. Phys. 82 (1985) 299–310.
[27] W.R. Wadt, P.J. Hay, J. Chem. Phys. 82 (1985) 284–298.
[28] C.E. Check, T.O. Faust, J.M. Bailey, B.J. Wright, T.M. Gilbert, L.S. Sunderlin, J. Phys. Chem. 105 (2001) 8111–8116.
[29] A. Ehlers, M. Böhme, S. Dapprich, A. Gobbi, A. Höllwarth, V. Jonas, K. Köhler, R. Stegmann, A. Veldkamp, G. Frenking, Chem. Phys. Lett. 208 (1993) 111–114.
[30] A. Höllwarth, M. Böhme, S. Dapprich, A. Ehlers, A. Gobbi, V. Jonas, K. Köhler, R. Stegmann, A. Veldkamp, G. Frenking, Chem. Phys. Lett. 208 (1993) 237–240.
[31] P.C. Hariharan, J.A. Pople, Theor. Chim. Acta 28 (1973) 213–222.
[32] M.S. Gordon, Chem. Phys. Lett. 76 (1980) 163–168.
[33] R. Binning, L. Curtiss, J. Comput. Chem. 11 (1990) 1206–1216.
[34] A.D. Becke, J. Chem. Phys. 98 (1993) 5648–5652.
[35] A.V. Marenich, C.J. Cramer, D.G. Truhlar, J. Phys. Chem. B 113 (2009) 6378–6396.
[36] T. Lu, F. Chen, Acta Chim. Sin. 69 (2011) 2393–2406.
[37] C.S. Letko, J.A. Panetier, M. Head-Gordon, T.D. Tilley, J. Am. Chem. Soc. 136 (2014) 9364–9376.